Amyloid Fibrils

DOI: 10.1002/ange.201403815

Cold Denaturation of α-Synuclein Amyloid Fibrils**

*Tatsuya Ikenoue, Young-Ho Lee, József Kardos, Miyu Saiki, Hisashi Yagi, Yasushi Kawata, and Yuji Goto**

Abstract: *Although amyloid fibrils are associated with numerous pathologies, their conformational stability remains largely unclear. Herein, we probe the thermal stability of various amyloid fibrils. α-Synuclein fibrils cold-denatured to monomers at 0–20°C and heat-denatured at 60–110°C. Meanwhile, the fibrils of β2-microglobulin, Alzheimer's Aβ1-40/Aβ1-42 peptides, and insulin exhibited only heat denaturation, although they showed a decrease in stability at low temperature. A comparison of structural parameters with positive enthalpy and heat capacity changes which showed opposite signs to protein folding suggested that the burial of charged residues in fibril cores contributed to the cold denaturation of α-synuclein fibrils. We propose that although cold-denaturation is common to both native proteins and misfolded fibrillar states, the main-chain dominated amyloid structures may explain amyloid-specific cold denaturation arising from the unfavorable burial of charged side-chains in fibril cores.*

To examine the thermal sensitivity of amyloid fibrils, we first prepared the two types of mature α-synuclein (αSN) fibrils. Ultrasonication generated homogeneous fibrils shorter than the fibrils formed by stirring at 37°C (see Text 1 in the Supporting Information). The formation and conformational properties of fibrils were confirmed by thioflavin T (ThT) fluorescence (Figure S1A in the Supporting Information), far-UV circular dichroism (CD; Figure S1B), and atomic force microscopy (AFM; Figure 1B,C).

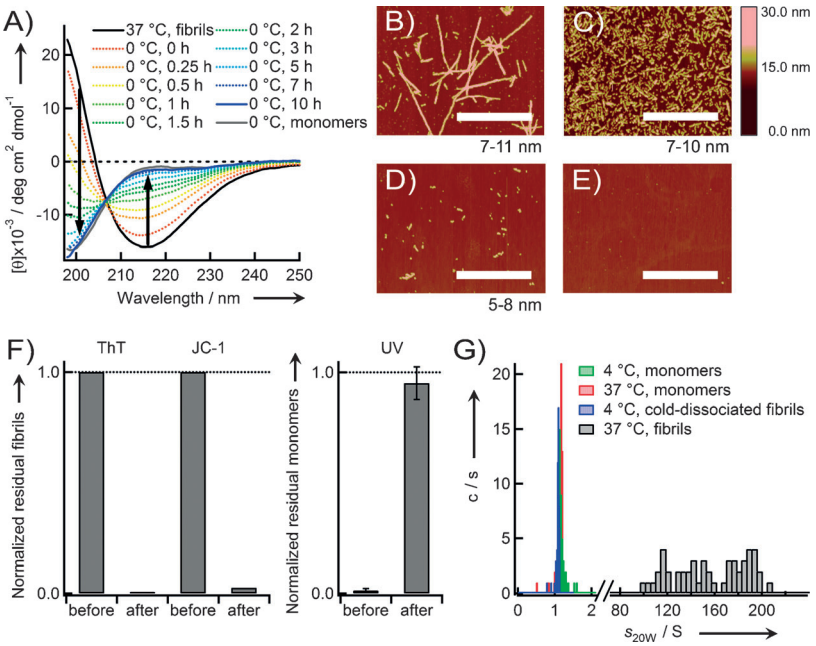

Figure 1. A) Cold denaturation of αSN fibrils monitored at 0°C by far-UV CD. The spectra of fibrils before (black) and after the cold treatment for 10 h (blue) and the spectrum of monomers at 0°C (gray). The changes on dissociation are shown by arrows. B),C) AFM images of αSN fibrils. Fibrils formed using stirring (B) or sonication (C). D),E) Fibrils after the cold treatment for 6 h at 10°C (D) and for 14 h at 0°C (E). Scale bars indicate 1 μm and average heights are exhibited at the right. F) Amounts of fibrils and monomers before and after the cold treatment at 0°C for 14 h. G) Fractions of molecular species against the S values ($s_{20,w}$).

The temperature was decreased from 37 to 0°C and conformational changes of αSN fibrils were monitored using far-UV CD (Figure 1A). The CD signal at approximately 218 nm decreased with incubation time. The spectrum after a 10 h incubation was essentially the same as that of the monomers at 0°C. Cold-treated fibril solutions showed no ThT or 5,5′,6,6′-tetrachloro-1,1′,3,3′-tetraethyl benzimidazolylcarbocyanine iodide (JC-1) fluorescence[1] at 485 nm or at 540 nm, respectively (Figure 1F), and no large molecules, such as residual fibrils and oligomers, were present in AFM images and analytical ultracentrifugation results (Figure 1E and G), indicating their almost complete denaturation to monomers, that is, cold denaturation (see Text 2 in the Supporting Information).

[*] T. Ikenoue,[+] Prof. Dr. Y.-H. Lee,[+] Prof. Dr. H. Yagi,[§] Prof. Dr. Y. Goto
Institute for Protein Research, Osaka University
3-2 Yamadaoka, Suita, Osaka 565-0871 (Japan)
E-mail: ygoto@protein.osaka-u.ac.jp
Prof. Dr. J. Kardos
Department of Biochemistry, Eötvös Loránd University, and MTA-ELTE-NAP B Neuroimmunology Research Group
1117 Budapest (Hungary)
M. Saiki, Prof. Dr. Y. Kawata
Department of Chemistry and Biotechnology, Graduate School of Engineering, Tottori University, 680-8552 Tottori (Japan)
[§] Current address: Department of Chemistry and Biotechnology, Graduate School of Engineering, and Center for Research on Green Sustainable Chemistry, Tottori University, 680-8552 Tottori (Japan)
[+] These authors contributed equally to this work.

[**] We thank Dr. Kazumasa Sakurai (Kinki University) for helping analytical ultracentrifugation measurements and Kyoko Kigawa (Osaka University) for preparing β_2m and αSN. This work was supported by the Japanese Ministry of Education, Culture, Sports, Science and Technology.

Supporting information for this article is available on the WWW under http://dx.doi.org/10.1002/anie.201403815.

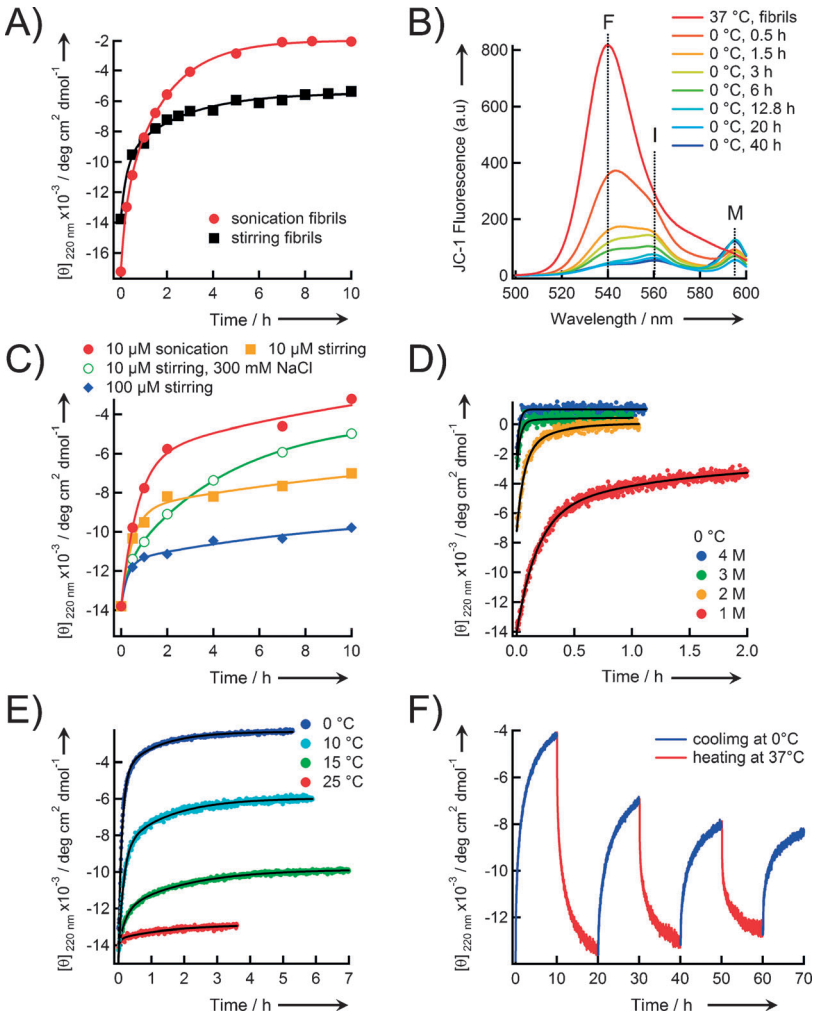

Figure 2. A) Time-dependent conformational changes in αSN fibrils at 0 °C. B) The JC-1 fluorescence spectrum at 0 °C. "F" = mature fibrils, "I" = intermediate fibrils, and "M" = monomers. C) The cold denaturation of fibrils at different salt or protein concentrations at 5 °C. D),E) The cold denaturation without (D) and with Gdn-HCl (E) at 0 °C. F) Reversibility of cold denaturation in the repeated cycles.

To explore the process of cold denaturation, the time course of changes in the CD signal at 220 nm was monitored at pH 7.4 and 0 °C (Figure 2 A). Time-dependent decreases in the amplitudes fit well with a double exponential function with the rate constants of fast (k_1) and slow (k_2) phases (see Text 3 in the Supporting Information). The average k_1 and k_2 values for short fibrils prepared using sonication were $5.29 \pm 0.75\ h^{-1}$ and $0.70 \pm 0.04\ h^{-1}$, respectively, with similar relative amplitudes (Table S1), suggesting a three-state mechanism with a kinetic intermediate state (i.e., protofibrils, see below) characterized using JC-1 fluorescence (Figure 2 B) and AFM images (Figure 1 B–E) (see Text 4 in the Supporting Information). The slower rates of biphasic cold denaturation of longer fibrils suggested that cold denaturation mainly occurs from the ends of fibrils and that ultrasonication increased the number of active sites of denaturation (see Text 5 in the Supporting Information).

It was found that cold denaturation was also susceptible to physicochemical factors (Figure 2 C–E). Increasing the sodium chloride and protein concentration delayed cold denaturation and increasing guanidine hydrochloride (Gdn-HCl) and temperature lead to adverse effects (see Tex 5 in the Supporting Information). Observation of oligomeric species in cold-treated αSN fibril solutions with high αSN concentrations (ca. 100–200 μM)[2] can be explained by kinetically trapped intermediate states. Much lower temperatures below the freezing point, such as 15 °C, effectively result in cold denaturation to monomers, even at high protein concentrations.[3] Thus, cold denaturation is an additional factor that determines the stability of fibrils, which is dependent on solvent conditions and αSN concentrations.

Note that the partial reversibility of the cold denaturation of αSN fibrils was verified by regenerating fibrils after cold denaturation by jumping the temperature to 37 °C followed by jumping the temperature to 0 °C to achieve cold denaturation (Figure 2 F, and Figures S2A,B). Interestingly, although regenerated fibrils again exhibited cold denaturation, the denaturation rate appeared to be slower. As the cycle of heating and cooling was repeated, reversibility declined with an apparent resistance to cold denaturation. This may have happened as a result of an adaptation to cold denaturation and/or the formation of irreversible aggregates of fibrils thereby weakening the efficiency of the fibrillation transition (see Text 6 in the Supporting Information).

Then, thermal responses of αSN fibrils over a wide temperature range (37–110 °C) were examined (Figure 3). CD intensities at 220 nm increased rapidly and saturated to an equilibrium point within 0.2 h (Figure 3 A), which revealed that heat denaturation was much faster than cold denaturation. The CD spectra measured after incubation at each temperature revealed the temperature-dependent heat denaturation of fibrils (Figure 3 B). The CD signal decreased with an increase in temperature and the spectrum at 110 °C was indistinguishable from that of monomers at 110 °C. These results indicate heat denaturation of fibrils to monomers, which is consistent with our previous study.[4] The thermal reversibility depended on the final heating temperature, fibril seeds, and the partial formation of irreversible aggregates (see Text 7 in the Supporting Information).

Interestingly, when the denaturation of fibrils was monitored by differential scanning calorimetry (DSC), the heat capacity exhibited a negative peak and no reversibility was observed after heating to 125 °C (Figure 3 D). The negative peak was opposite to the typical positive heat-capacity peak accompanied by the unfolding of globular proteins,[5] which suggested a positive enthalpy change in αSN fibril formation.

To extract the general features of the temperature responses of amyloid fibrils, fibrils of various amyloidogenic

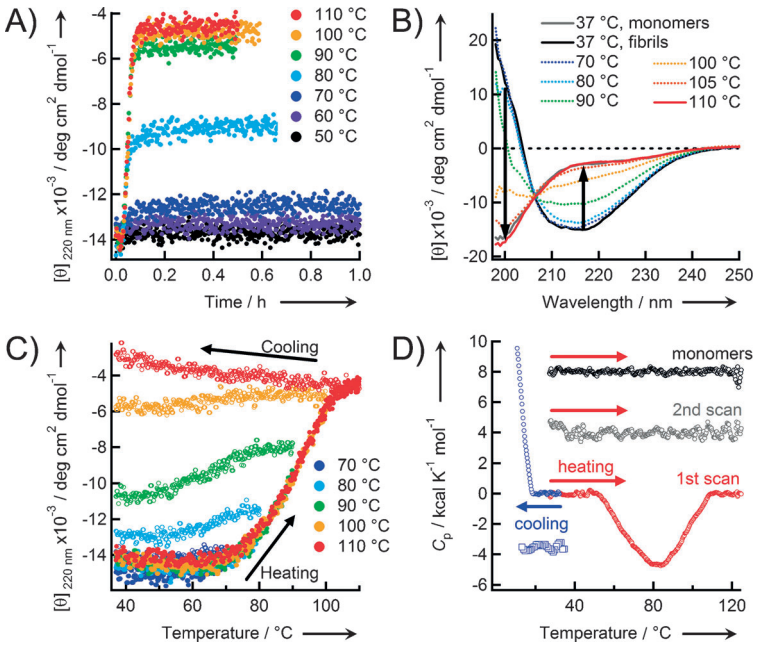

Figure 3. A) The kinetics of the thermal denaturation of αSN fibrils. B) CD spectra of αSN fibrils at 37 °C after the heat treatment. The changes on heat treatment are indicated by the arrows. C),D) The heat denaturation of fibrils observed by CD (C) or DSC (D). The arrows indicate the direction of scanning. C) The final temperature of each thermal scan was 70, 80, 90, 100, or 110 °C. D) The C_p curves of αSN fibrils (○) and monomers (○) and of the second heat scan of αSN fibrils (○). The DSC thermograms of αSN (○) and β_2m fibrils (□).

proteins under different solvent conditions were examined (Figure 4). A bell-shaped thermal stability curve of αSN fibrils explained the temperature-dependent conformational stability of amyloid fibrils in a two-state transition between fibrils and monomers at low and high temperature (Figure 4A). Fibrils were stable between 25 and 60 °C, however, they were unstable below 25 °C and above 60 °C. The apparent midpoints at which 50% of fibrils depolymerized were 12 and 91 °C for cold and heat denaturation, respectively (Table S2).

Bell-shaped symmetric stability curves were also obtained for fibrils of αSN mutants formed at 37 °C and pH 7.4: αSN_{118} (Met1 to Val118), αSN_{103} (Met1 to Asn103), $NAC_{76\text{-}96}$ (Ala76 to Lys96), and E83Q (substitution of Glu to Gln) (Figure 4B). Considering the possible role of buried charges in the core of fibrils (see below), we also examined the thermal denaturation at pH 2.5. Interestingly, no significant cold denaturation of fibrils of full-length αSN, αSN_{103}, and αSN_{118} was observed at 0 °C (Figure 4B).

Although mature β2-microglobulin (β_2m) and K3 fibrils, the three types of fibrils of amyloid $\beta(A\beta)_{1\text{-}42}$ and $A\beta_{1\text{-}40}$ peptides, and insulin fibrils showed only heat denaturation, thin and curved immature β_2m fibrils showed cold denaturation with approximately 15% of fibrils remaining at 0 °C (Figure 4C and D).

Then, the effects of Gdn-HCl on the stability of fibrils at different temperatures were examined to address the relationship between the chemical, cold, and heat stabilities of fibrils (see Text 8 in the Supporting Information). Using either CD or ThT fluorescence, ten different fibrils were observed to denature completely at a high Gdn-HCl concentration (Figure S3 and Table S2). Lowering the temperature to 0 °C enhanced Gdn-HCl-induced denaturation of αSN fibrils formed at pH 2.5 and $A\beta_{1\text{-}42}/A\beta_{1\text{-}40}$ fibrils with decreasing the apparent midpoint Gdn-HCl concentration (C_m). These results indicate that the effects of Gdn-HCl and low temperature are additive, with both destabilizing amyloid fibrils.

The thermodynamic parameters associated with fibril growth, which provide key indications toward understanding the mechanism of fibrillation, were characterized using calorimetry. The seed-dependent growth of K3 and $A\beta_{1\text{-}40}$ fibrils was accompanied by the release of heat in accordance with our previous results for β_2m fibril elongation (Figure 5A).[6] Interestingly, αSN fibril extension was accompanied by heat absorption. The apparent values of the enthalpy change (ΔH) for K3, β_2m, $A\beta_{1\text{-}40}$, and αSN fibril growth (pH 7.4) were −10.2, −28.5, −36.8, and +8.8 kcal mol^{-1} at 37 °C, respectively (Table S3).

The positive ΔH for the αSN fibrillation was consistent with the negative heat capacity peak observed upon heat denaturation of αSN fibrils by DSC (Figure 3D). The change in heat capacity (ΔC_p) was shown to be 0.35 kcal mol^{-1} K^{-1} (Figure 5B). This value was positive while those of the fibrillation and folding of β_2m were −1.14 and −1.34 kcal mol^{-1} K^{-1}, respectively (Table S3). The decrease in pH value from 7.4 to 2.5 inversed the signature of ΔH and ΔC_p for the αSN fibril growth (Figure 5B). The predicted ΔC_p value for protein folding of globular proteins was −1.56 K^{-1} for β_2m and that for αSN was −2.3 kcal mol^{-1} K^{-1} on the assumption that aSN, an intrinsically disordered protein, folds. This result showed that the empirical relationship on the basis of protein folding did not necessarily apply to protein misfolding. The inverse sign of ΔH and ΔC_p raised questions about energetic contributions to the stability of αSN fibrils inferred from other fibrils and protein folding.

All of the fourteen fibrils examined exhibited heat denaturation as well as Gdn-HCl denaturation. The T_m, C_m, and m values obtained were in similar ranges to those of globular proteins (Figure 4 and Figure 5, Table S2),[7] which suggests that the stabilities of amyloid fibrils are not very different from those of globular proteins.[8]

Based on the results obtained, we addressed the molecular origin of the cold denaturation of αSN fibrils. Cold denaturation of fibrils formed by charge-deleted mutants (αSN_{103} and αSN_{108}) and hydrophobic NAC peptide at pH 7.4 raised a possible role for the charged residues at pH 7.4 (K43(+), K45(+), E46(−), H50(+), E57(−), K58(+), K60(+), E61(−), K80(+), E83(−), K96(+), K97(+), and D98(−)) buried in fibril cores (Figure 4B, Table S4) without forming fully satisfied electrostatic networks. Accordingly, full-length αSN fibrils were prepared at pH 2.5 at which negatively charged residues are protonated. No significant cold denaturation was

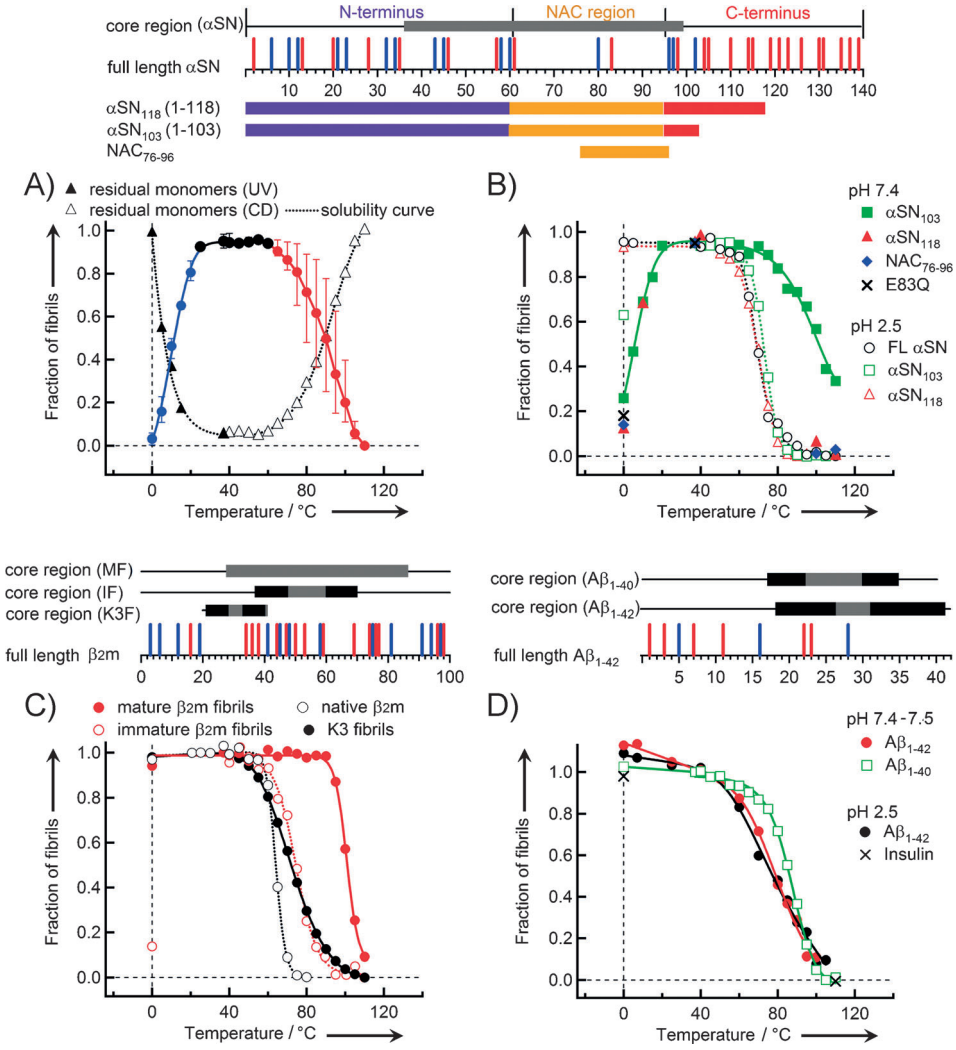

Figure 4. A) Temperature-dependent fractions of fibrils of full-length αSN at pH 7.4. The unstable temperature regions of fibrils against cold (●) and heat (●) and the stable region (●). The solubility curve of αSN determined by UV-visible (▲) or CD (△) spectra. B) Thermal stability curves of various αSN fibrils. The amphipathic N-terminal (blue), hydrophobic NAC (yellow), and hydrophilic C-terminal regions (red) of αSN are depicted at the top. C) Thermal stability curves of the remaining β_2m and K3 fibrils and the fractions of native β_2m monomers. D) Thermal stability curves of fractions of $A\beta_{1\text{-}42}$, $A\beta_{1\text{-}40}$, and insulin fibrils. The negatively and positively charged residues of corresponding monomers at neutral pH values are shown by red and blue bars, respectively. Core regions and β-strands in fibrils (Table S4) are signified by gray and black rectangles, respectively. All continuous lines are to guide the eye.

observed when full-length αSN, αSN_{103}, and αSN_{108} fibrils formed at pH 2.5 were incubated at 0 °C.

Therefore, the unfavorable burial of the negative charges in cores at neutral pH value may be responsible for the cold denaturation of αSN fibrils because electrostatic repulsion becomes stronger with a decrease in temperature owing to the increases in the dielectric constant[9] and in hydrophobic hydration.[10] This view can be further supported by the findings that charge repulsion following the pH changes unfolds amyloid fibrils[11] and even a single charge buried in a hydrophobic core readily dissociates fibrils.[12] High packing density and hydrophobic burial with complementary pairs of buried polar groups are key ingredients of protein stability.[13]

Most importantly, the positive values of ΔH and ΔC_p observed for αSN fibrils by ITC and DSC were opposite to those of protein folding and other cases of protein misfolding reactions,[5–7,10] arguing strongly for the burial of charges as evidenced by the positive ΔC_p value following dehydration of charged residues.[14] Such adverse changes of ΔH and ΔC_p were also detected in DNA–protein,[15] nucleotide–protein,[16] lipid bilayer–protein,[17] and the anion–protein binding[18] systems as well as and DNA condensation[19] in which charges were buried upon complexation. The recent study also indicated that the unstable glucagon fibrils formed with large positive ΔH and ΔC_p values was attributed to the possible unfavorable burial of polar and/or charged residues.[20]

However, fibrils of αSN mutant (E83Q) showed cold denaturation at pH 7.4 (Figure 4B), which suggested that the charge burial of E83 did not occur in forming fibrils or that buried charges formed satisfactory electrostatic networks. Alternatively, it may suggest the involvement of an additional factor in the cold denaturation of αSN fibrils. Although the unfavorable burial of a negative charge among E46, E57, E61, and D98 in the cores may have been responsible for the cold denaturation of αSN fibrils, cold denaturation of immature β_2m fibrils and Gdn-HCl-promoted cold denaturation of $A\beta_{1\text{-}40}$/$A\beta_{1\text{-}42}$ fibrils and αSN fibrils at pH 2.5 suggest that cold denaturation is common phenomenon to amyloid fibrils even in the absence of unique burial of charged groups as shown with a high positive correlation ($R = 0.83$ and $p < 0.01$) between the fraction of fibrils at 0 °C and the C_m value of the Gdn-HCl-induced denaturation (Figure 5F).

The lack of significant correlations between the fraction of fibrils at 0 °C and net charge, hydrophobicity, or ΔH suggests that there are currently no clear mechanisms to explain the cold denaturation of fibrils based on protein (un)folding (Figure 5C and D, Figure S4A). Nevertheless, a strong negative correlation between the fraction of fibrils at 0 °C and protein solubility ($R = -0.9$ and $p < 0.014$; Figure 5E) implies that fibrils with a propensity to cold-denature are those with intrinsically high solubility. When proteins with intrinsically

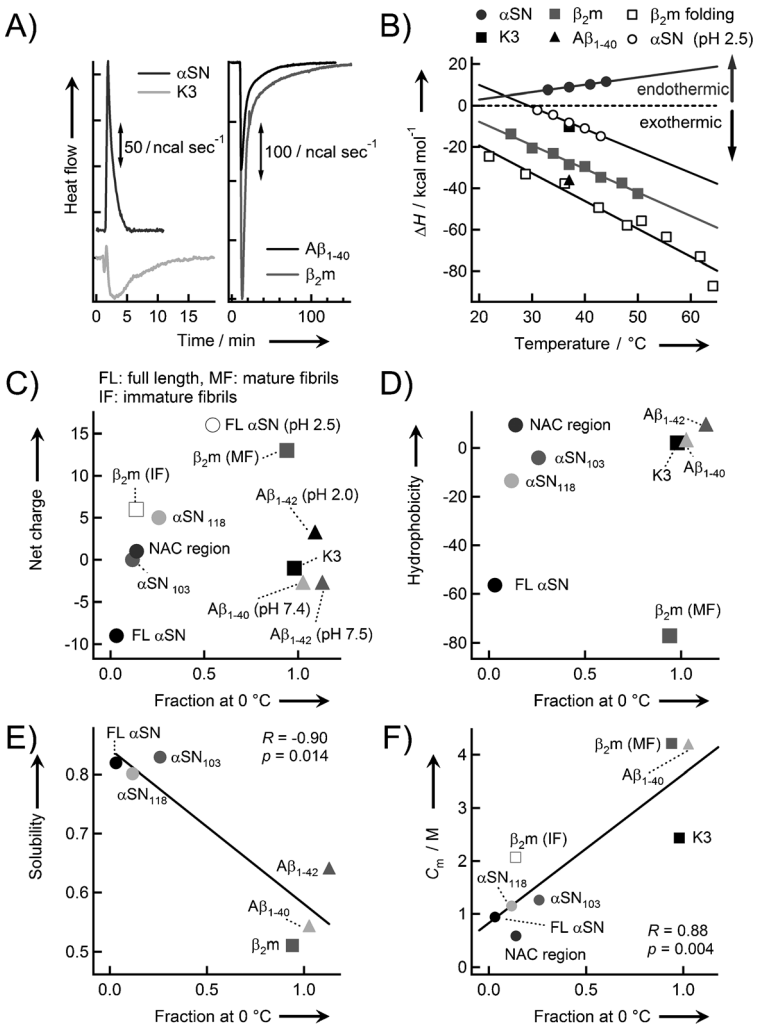

Figure 5. A) Fibril elongations at 37 °C observed using ITC. B) Temperature-dependent changes in ΔH for the fibril growths and folding of β_2m. C–F) Net charge (C), hydrophobicity (D), and solubility (E) of amyloidogenic monomers as well as C_m values of various amyloid fibrils (F) plotted against the fractions of remaining fibrils at 0 °C. A correlation coefficient R value is shown.

high solubility form fibrils at ambient temperatures by overcoming solubility and taking advantage of the main-chain dominated architecture, they are more likely to be disassembled at low temperatures. Such amyloid fibrils may be detected by the decreased or positive ΔH value together with the positive ΔC_p value of fibrillation (Figure S4A,B).

The overall process for the thermal responses of αSN fibrils was drawn schematically in Figure 6. Mature αSN fibrils are stable (20–60 °C), as the temperature decreases below 20 °C, fibrils begin to denature to monomers through a thin fibrillar intermediate, which may be formed by the dissociation of mature fibrils without axial fibril breakage. Dissociation of mature prion protein fibrils by charge repulsion into protofilaments may reflect similar lateral dissociation behavior of mature αSN fibrils.[11d] The driving force for the cold denaturation of αSN fibrils is the entropy-driven solvation of residues from the interior of fibrils based on amyloid-specific thermodynamics of the enthalpic penalty of the endothermic reaction and increase in heat capacity. On the other hand, heat denaturation was observed for all the fibrils examined. The thermodynamic driving force of depolymerization at high temperatures may be conformational entropy, similar to the unfolding of globular proteins at high temperatures.

Finally, in contrast to solid formation above the critical concentration, increases in solubility below the critical concentration dissociate solid states.[21] Accordingly, the conformational stability of amyloid fibrils can be defined by solubility,[4,6,8,21] which is the amount of remaining soluble monomers in equilibrium with fibrils. This provides a simple, but understandable concept that fibril stability can be determined by the thermodynamic solubility of monomers without considering complicated mechanisms, although kinetic stability is limited by ambient conditions. Mature αSN fibrils formed at pH 7.4 showed a unique U-shaped solubility curve in the temperature range of 0 to 110 °C, which was an exact inverse pattern of the stability of αSN fibrils (Figure 4 A). We consider that the cold-denaturation phenomena observed in this case were also coupled with the increased solubility at low temperatures.

Combining the viewpoints of solubility, crystalline amyloid fibrils limited by supersaturation, and glass-like amorphous aggregates, we can make further understanding of the thermodynamic mechanism of protein fibrillation. Furthermore, our results also provide biological implications for αSN protein homeostasis. The disaggregation and clearance of αSN aggregates should be easier to achieve than those of Aβ, β2m, and insulin fibrils taking advantage of the marked propensity for cold-denaturation of αSN fibrils even near the physiological temperatures by increasing protein turnover. However cold adaptation may impede efficient αSN protein homeostasis.

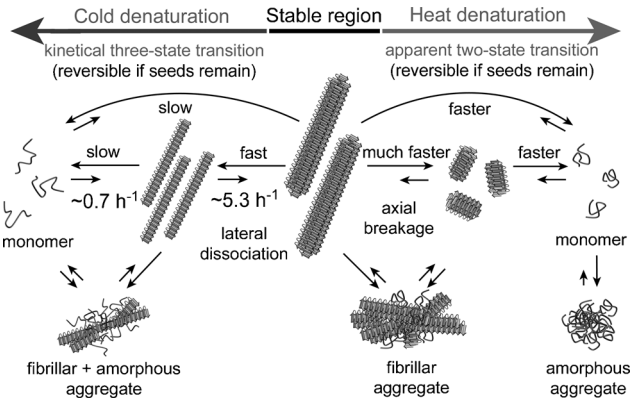

Figure 6. Schematic mechanism of the cold and heat denaturation of αSN fibrils.

Experimental Section

Preparation of proteins and fibrils: The recombinant full-length human αSN and β_2m and the two αSN mutants, αSN_{103}, αSN_{118}, and

E83Q were expressed in *Escherichia coli* strain BL21 (DE3) and BLR (DE3) (Novagen, Madison, WI), respectively, and were purified as described elsewhere.[4,6,22] The K3 peptide was obtained by the digestion of β_2m with *Acromobacter* protease I. NAC_{76-96} and $A\beta_{1-40}$ peptide were purchased from Peptide Institute Inc. (Osaka, Japan). $A\beta_{1-42}$ was expressed and purified as described in the Supporting Information. Insulin was purchased from Wako Pure Chemical Industries Ltd (Osaka, Japan). Seed-dependent fibrillation of all proteins and peptides was described in Text 1 in the Supporting Information. All cold and heat denaturation-related measurements are described in the Supporting Information.

Received: March 29, 2014
Published online: June 11, 2014

Keywords: aggregation · amyloid fibrils · calorimetry · denaturation · protein misfolding

[1] J. H. Lee, I. H. Lee, Y. J. Choe, S. Kang, H. Y. Kim, W. P. Gai, J. S. Hahn, S. R. Paik, *Biochem. J.* **2009**, *418*, 311 – 323.
[2] a) H. Y. Kim, M. K. Cho, A. Kumar, E. Maier, C. Siebenhaar, S. Becker, C. O. Fernandez, H. A. Lashuel, R. Benz, A. Lange, M. Zweckstetter, *J. Am. Chem. Soc.* **2009**, *131*, 17482 – 17489; b) L. Bousset, L. Pieri, G. Ruiz-Arlandis, J. Gath, P. H. Jensen, B. Habenstein, K. Madiona, V. Olieric, A. Bockmann, B. H. Meier, R. Melki, *Nat. Commun.* **2013**, *4:2575* doi: 10.1038/ncomms3575.
[3] a) H. Y. Kim, M. K. Cho, D. Riedel, C. O. Fernandez, M. Zweckstetter, *Angew. Chem.* **2008**, *120*, 5124 – 5126; *Angew. Chem. Int. Ed.* **2008**, *47*, 5046 – 5048; b) R. Mishra, R. Winter, *Angew. Chem.* **2008**, *120*, 6618 – 6621; *Angew. Chem. Int. Ed.* **2008**, *47*, 6518 – 6521.
[4] J. Kardos, A. Micsonai, H. Pal-Gabor, E. Petrik, L. Graf, J. Kovacs, Y. H. Lee, H. Naiki, Y. Goto, *Biochemistry* **2011**, *50*, 3211 – 3220.
[5] P. L. Privalov, *Pure Appl. Chem.* **2007**, *79*, 1445 – 1462.
[6] J. Kardos, K. Yamamoto, K. Hasegawa, H. Naiki, Y. Goto, *J. Biol. Chem.* **2004**, *279*, 55308 – 55314.
[7] J. K. Myers, C. N. Pace, J. M. Scholtz, *Protein Sci.* **1995**, *4*, 2138 – 2148.
[8] a) T. Narimoto, K. Sakurai, A. Okamoto, E. Chatani, M. Hoshino, K. Hasegawa, H. Naiki, Y. Goto, *FEBS Lett.* **2004**, *576*, 313 – 319; b) A. J. Baldwin, T. P. Knowles, G. G. Tartaglia, A. W. Fitzpatrick, G. L. Devlin, S. L. Shammas, C. A. Waudby, M. F. Mossuto, S. Meehan, S. L. Gras, J. Christodoulou, S. J. Anthony-Cahill, P. D. Barker, M. Vendruscolo, C. M. Dobson, *J. Am. Chem. Soc.* **2011**, *133*, 14160 – 14163.
[9] S. Kumar, R. Nussinov, *ChemBioChem* **2004**, *5*, 280 – 290.
[10] C. L. Dias, T. Ala-Nissila, J. Wong-ekkabut, I. Vattulainen, M. Grant, M. Karttunen, *Cryobiology* **2010**, *60*, 91 – 99.
[11] a) R. P. McGlinchey, J. M. Gruschus, A. Nagy, J. C. Lee, *Biochemistry* **2011**, *50*, 10567 – 10569; b) S. L. Shammas, T. P. Knowles, A. J. Baldwin, C. E. Macphee, M. E. Welland, C. M. Dobson, G. L. Devlin, *Biophys. J.* **2011**, *100*, 2783 – 2791; c) P. Picotti, G. De Franceschi, E. Frare, B. Spolaore, M. Zambonin, F. Chiti, P. P. de Laureto, A. Fontana, *J. Mol. Biol.* **2007**, *367*, 1237 – 1245; d) X. Qi, R. A. Moore, M. A. McGuirl, *Biochemistry* **2012**, *51*, 4600 – 4608.
[12] T. J. Measey, F. Gai, *Langmuir* **2012**, *28*, 12588 – 12592.
[13] K. A. Dill, S. B. Ozkan, M. S. Shell, T. R. Weikl, *Annu. Rev. Biophys.* **2008**, *37*, 289 – 316.
[14] a) N. V. Prabhu, K. A. Sharp, *Annu. Rev. Phys. Chem.* **2005**, *56*, 521 – 548; b) S. Kumar, R. Nussinov, *ChemBioChem* **2002**, *3*, 604 – 617.
[15] S. H. Chen, C. K. Suzuki, S. H. Wu, *Nucleic Acids Res.* **2008**, *36*, 1273 – 1287.
[16] J. P. Robblee, W. Cao, A. Henn, D. E. Hannemann, E. M. De La Cruz, *Biochemistry* **2005**, *44*, 10238 – 10249.
[17] Y. K. Reshetnyak, O. A. Andreev, M. Segala, V. S. Markin, D. M. Engelman, *Proc. Natl. Acad. Sci. USA* **2008**, *105*, 15340 – 15345.
[18] M. Boncina, J. Lah, J. Rescic, V. Vlachy, *J. Phys. Chem. B* **2010**, *114*, 4313 – 4319.
[19] D. Matulis, I. Rouzina, V. A. Bloomfield, *J. Am. Chem. Soc.* **2002**, *124*, 7331 – 7342.
[20] M. D. Jeppesen, K. Hein, P. Nissen, P. Westh, D. E. Otzen, *Biophys. Chem.* **2010**, *149*, 40 – 46.
[21] a) R. Wetzel, S. Shivaprasad, A. D. Williams, *Biochemistry* **2007**, *46*, 1 – 10; b) J. T. Jarrett, P. T. Lansbury, Jr., *Cell* **1993**, *73*, 1055 – 1058.
[22] a) H. Yagi, H. Takeuchi, S. Ogawa, N. Ito, I. Sakane, K. Hongo, T. Mizobata, Y. Goto, Y. Kawata, *Biochim. Biophys. Acta Proteins Proteomics* **2010**, *1804*, 2077 – 2087; b) Y. Izawa, H. Tateno, H. Kameda, K. Hirakawa, K. Hato, H. Yagi, K. Hongo, T. Mizobata, Y. Kawata, *Brain Behav.* **2012**, *2*, 595 – 605.